

Supporting Information

Lead-Free Two-Dimensional Perovskite for High-Performance Flexible Photoconductor and Light-Stimulated Synaptic Device

Liu Qian,^{‡a,b,c} Yilin Sun,^{‡d} Mingmao Wu,^a Chun Li,^a Dan Xie,^{*d} Liming Ding,^{*b,c} Gaoquan

Shi^{*a}

^aDepartment of Chemistry, Key Laboratory of Bioorganic Phosphorus Chemistry & Chemical Biology (MOE), Tsinghua University, Beijing 100084, China. E-mail: gshi@tsinghua.edu.cn

^bCenter for Excellence in Nanoscience, Key Laboratory of Nanosystem and Hierarchical Fabrication (CAS), National Center for Nanoscience and Technology, Beijing 100190, China. E-mail: ding@nanoctr.cn

^cUniversity of Chinese Academy of Sciences, Beijing 100049, China.

^dTsinghua National Laboratory for Information Science and Technology (TNList), Institute of Microelectronics, Tsinghua University, Beijing 100084, China. E-mail: xiedan@tsinghua.edu.cn

1. Methods

GO Preparation: GO was prepared by a modified Hummers' method according to our previous literature.¹ Typically, graphite powder (3.0 g, 200 mesh, Qingdao Huatai Lubricant Sealing S&T Co., Ltd., China) was slowly added into concentrated sulfuric acid (72 mL, 98%) under mechanical stirring (300 rpm) at 0 °C. After 30 min stirring, potassium permanganate (9.0 g) was added slowly to maintain the reaction

temperature lower than 5 °C. Afterwards, the reaction suspension was stirred for 16 h below 5 °C. Deionized water (150 mL) was then added into the mixture by using a peristaltic pump. The final reaction mixture was poured into 500 mL of an ice water mixture and then 15 mL of hydrogen peroxide (30% aqueous solution) was dropwise added to terminate the reaction. Subsequently, the product was filtered and washed with 250 mL of aqueous HCl solution (3.7 wt%) and ample deionized water to remove metal ions. The resultant slurry was dispersed in deionized water (1200 mL) under vigorous stirring to form an aqueous GO dispersion. The resultant GO dispersion was subjected to dialysis (cut off of 8000–14 000 Da) for 15 days to remove the residual acid and metal impurities. Finally, the GO suspension was purified by centrifugation repeatedly at 2000 rpm for 20 min to remove unexfoliated graphite oxide particles, followed by concentration at 10 000 rpm for 60 min.

Preparation of Electrodes: The method for preparation of GO is given in the ESI†. PET substrates (0.125 mm) were cleaned ultrasonically in acetone, ethanol, and isopropyl alcohol for 20 min sequentially, dried by N₂-flow and followed by a 10 min UV-ozone treatment. The GO aqueous dispersion (1 mg mL⁻¹) was mixed with different volume percentage of PEDOT:PSS (PH1000) (30 ~ 70 vol%) by stirring for 2 h. The mixed solution was spin coated onto the PET substrates at 4000 rpm and baked at 120 °C for 10 min. The films were then processed with HI (55% w/w aqueous solution) overnight and rinsed by ethanol for three times. After that, the rGO/(PEDOT:PSS) composite films on PET substrate were spin-coated with negative

photoresist (NR9-3000PY) and patterned to be interdigital by a standard photolithographic procedure, including 90 s for exposure and another 90 s for photoresist post-baking followed by a 80s developing process in the developer solution (RD6). Then, the composite films out of the photoresist protection were removed by O₂ plasma etching process, in which the gas pressure and etching power was set to be 13 Pa and 100 W, respectively. After the three minute etching process, the residual photoresist was removed by acetone. The width of the finger was 10 μm and the spacing between neighboring fingers was also controlled to be 10 μm. The same size of interdigitated Au electrodes were prepared by a photolithography and lift-off method via successive evaporation deposition of 5 nm thick Cr (for enhancing the adhesion between the Au layer and PET) and 50 nm thick Au on PET substrates.

Device Fabrication: PEAI was prepared according to a previous literature.² A 2 : 1 ratio of PEAI/SnI₂ (Acros, 99.999%) was dissolved in N,N-dimethylformamide (Acros, 99.9%) and stirred for at least 3 h in a glovebox filled with argon gas. The concentration of the solution was 0.3 mol L⁻¹ with 0 mol% ~ 40 mol% SnF₂ addition. The solution was spin coated onto the interdigitated electrodes at 4000 rpm for 60 s and then heated at 90 °C for 10 min. The effective area of each device was 0.18 × 0.08 cm².

2. Characterization

UV-vis spectra and transmittance spectra were performed on a Lambda 35 UV-vis spectrometer (PerkinElmer). AFM images were recorded using a SPM-9600 scanning probe microscope (Shimadzu). XRD patterns were carried out on a Bruker D8 ADVANCE diffractometer with Cu K α ($\lambda = 1.5406 \text{ \AA}$) radiation. X-ray photoelectron spectra (XPS) were performed on an ESCALAB 250 photoelectron spectrometer (ThermoFisher Scientific) with Al K α (1486.6 eV) as the X-ray source set at 150 W and a pass energy of 30 eV for high-resolution scan. Raman and steady-state PL spectra were recorded on a LabRAM HR Evolution (Horiba Jobin Yvon) Raman spectrometer with a 532 nm laser. The ultraviolet photoelectron spectra (UPS) were obtained by using a Thermo Scientific ESCALab 250Xi UPS with a HeI lamp (21.22 eV). The TRPL spectra were taken out on a NanoLOG-TCSPC fluorescence spectrometer (Horiba Jobin Yvon) with monochromatic light at 515 nm. Scanning electron microscopy (SEM) images were obtained on a Sirion-200 field-emission scanning electron microscope.

The performance of the device was studied by using a Keithley 4200 SourceMeter. The monochromatic light with different wavelengths were provided by a CEL-LEDS35 light-emitting diode (LED) illuminant (CEAULIGHT). All measurements were performed in air at room temperature. The photoresponsivity (R) is defined as $R = (I_{\text{illumination}} - I_{\text{dark}})/(e \times S)$, where $I_{\text{illumination}}$ is the photocurrent under illumination, I_{dark} is the dark current, e is the incident irradiance, and S is the effective area of the device ($0.18 \text{ cm} \times 0.08 \text{ cm}$). Specific detectivity (D^*) of the device was calculated by using the equation of $D^* = S^{1/2}/\text{NEP} = S^{1/2}/(I_n/R)$, where NEP is the noise equivalent

power, I_n is the noise current in the unit of $A\ Hz^{-1/2}$; I_n was obtained by measuring the noise spectral density from the Fourier transform of current versus time.

3. Supplementary Figures

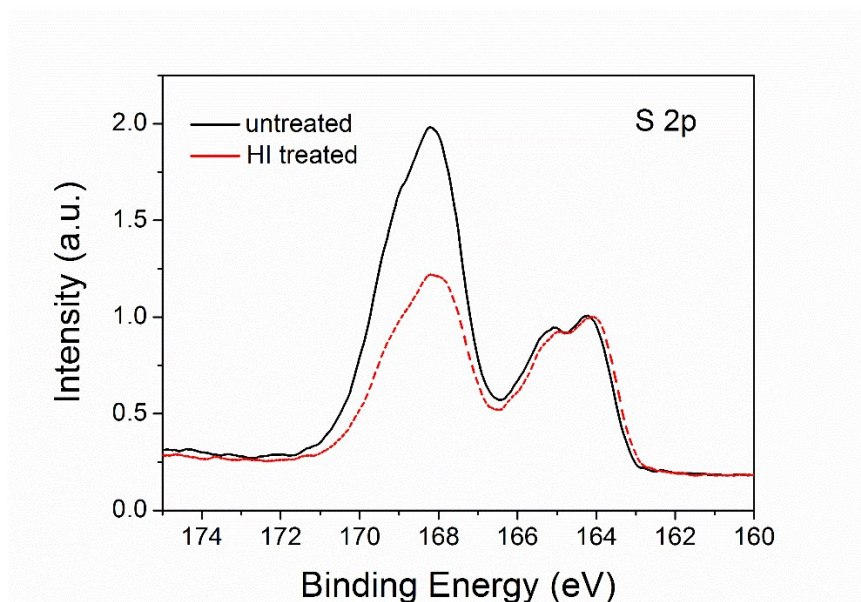


Fig. S1 S 2p XPS spectra of rGO/(PEDOT:PSS) films before and after the treatment with HI.

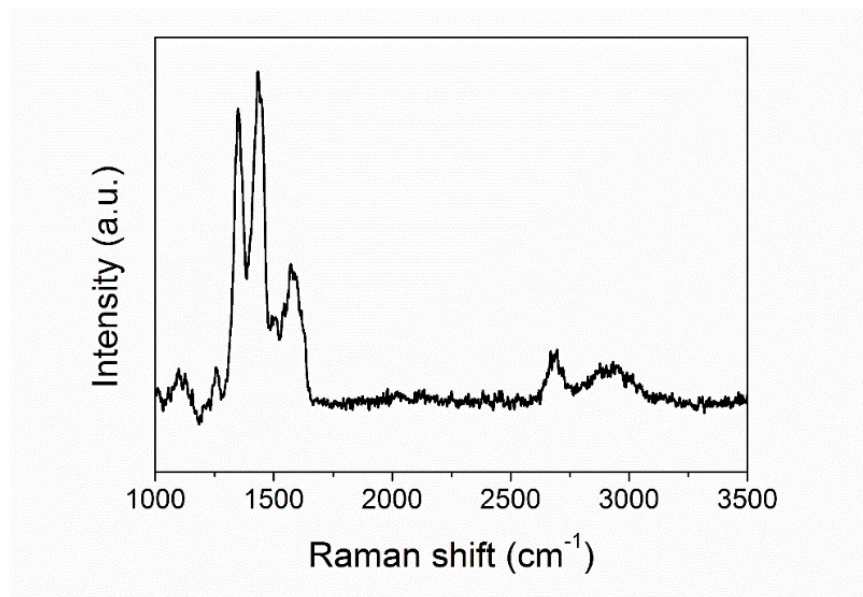


Fig. S2 Raman spectrum of as prepared rGO/(PEDOT:PSS) film.

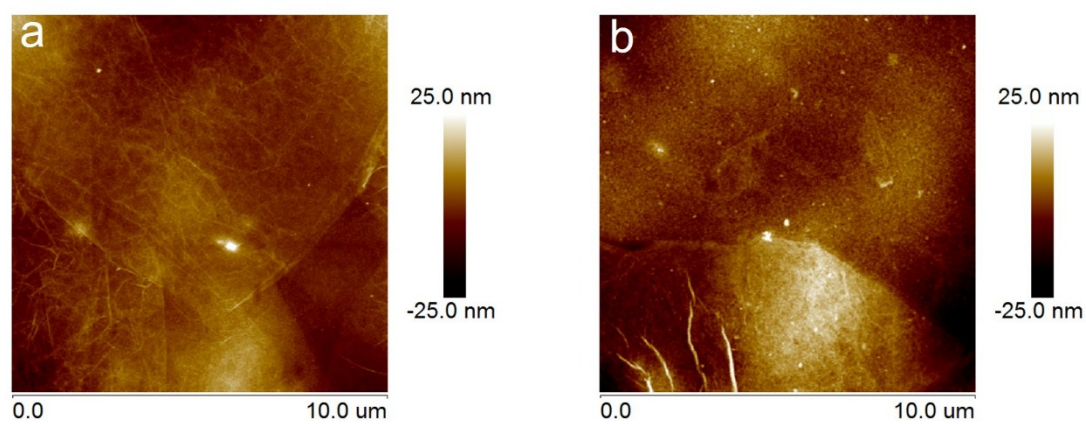


Fig. S3 AFM images of a) pristine rGO film and b) rGO-P60 film.

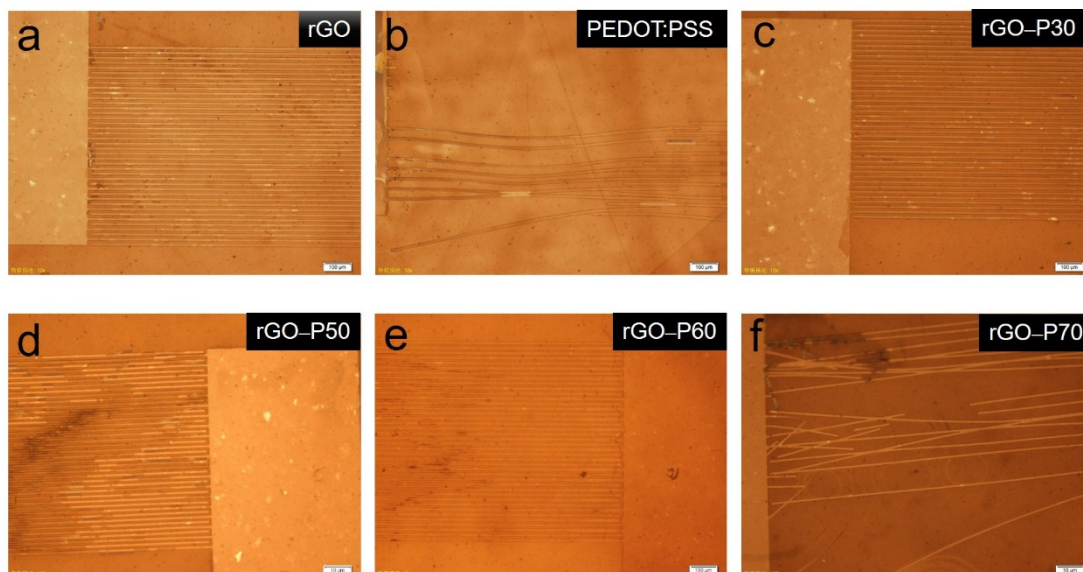


Fig. S4 Optical microscopy images of the interdigitated electrodes with different volume percentage of PEDOT:PSS. The scale bar is 100 μm .

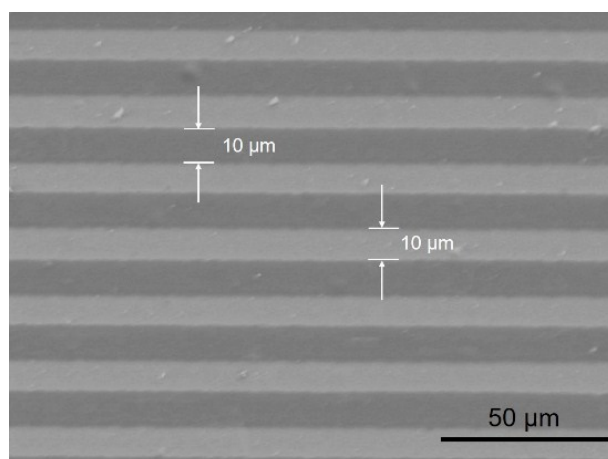


Fig. S5 SEM image of the electrode fingers.

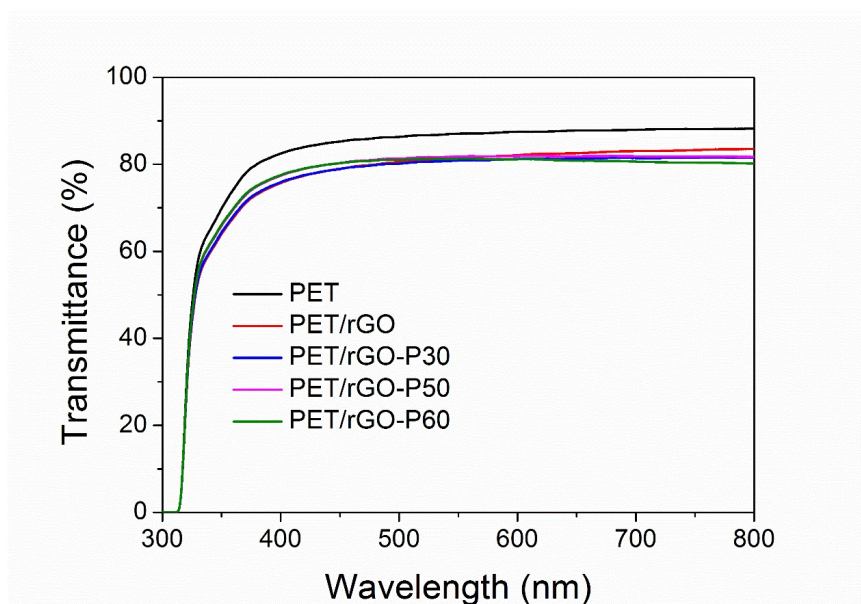


Fig. S6 Transmittance spectra of rGO/(PEDOT:PSS) film with PET substrate.

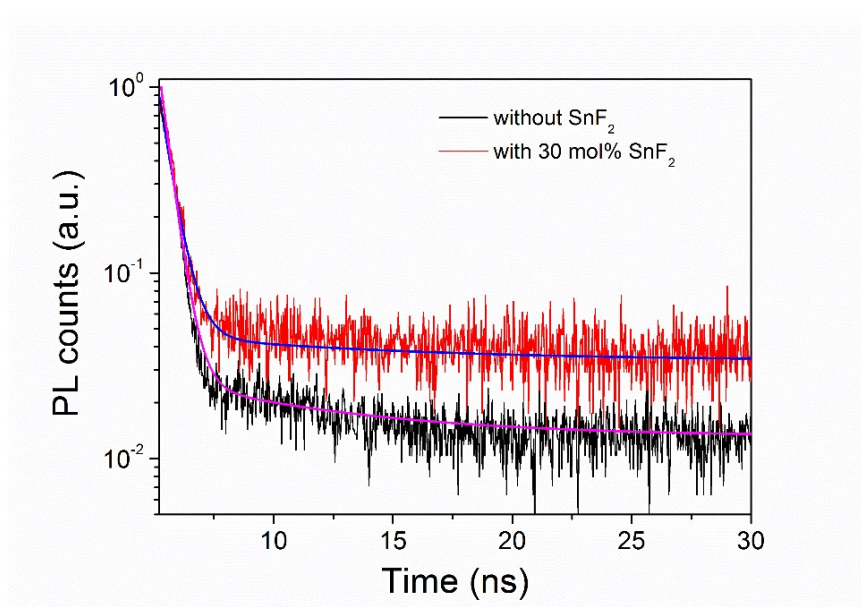


Fig. S7 Time-resolved photoluminescence decay and fitting curves of perovskite film without or with 30 mol% SnF_2 addition.

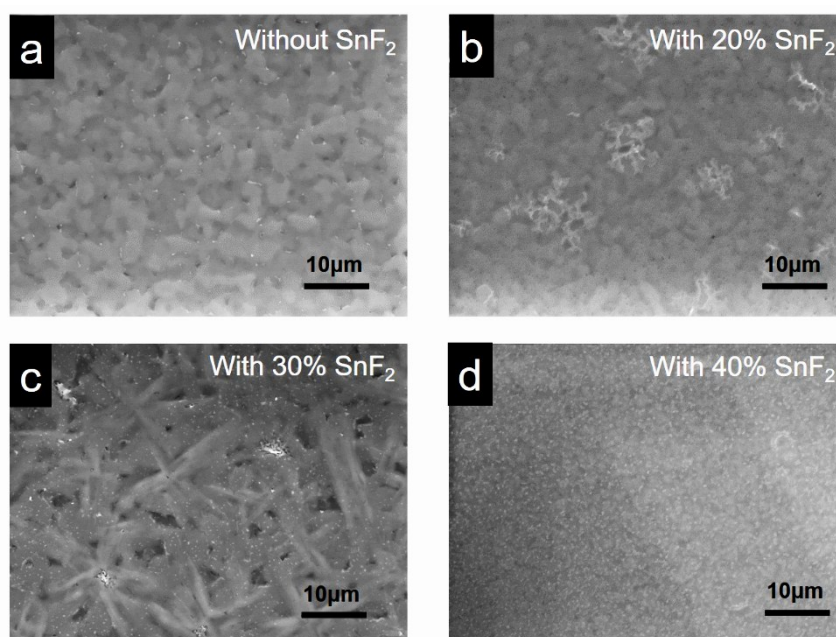


Fig. S8 Top view SEM images of perovskite film a) without or with b) 20 mol%, c) 30 mol% and d) 40 mol% addition of SnF_2 .

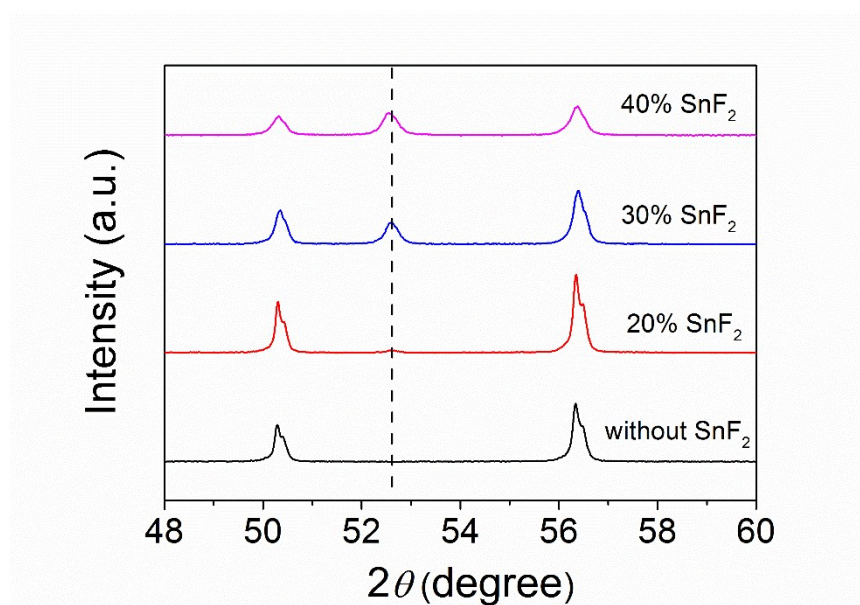


Fig. S9 Enlarged XRD patterns of perovskite films with different SnF_2 content.

Note: A new peak around 52.6° appeared when adding 20 mol% SnF_2 and the peak became stronger with the increase of SnF_2 amount. This peak may origin from the diffraction of some Sn-I-F phases. SnIF : JCPDS No. 23-1437; Sn_2IF_3 : JCPDS No. 23-1438.

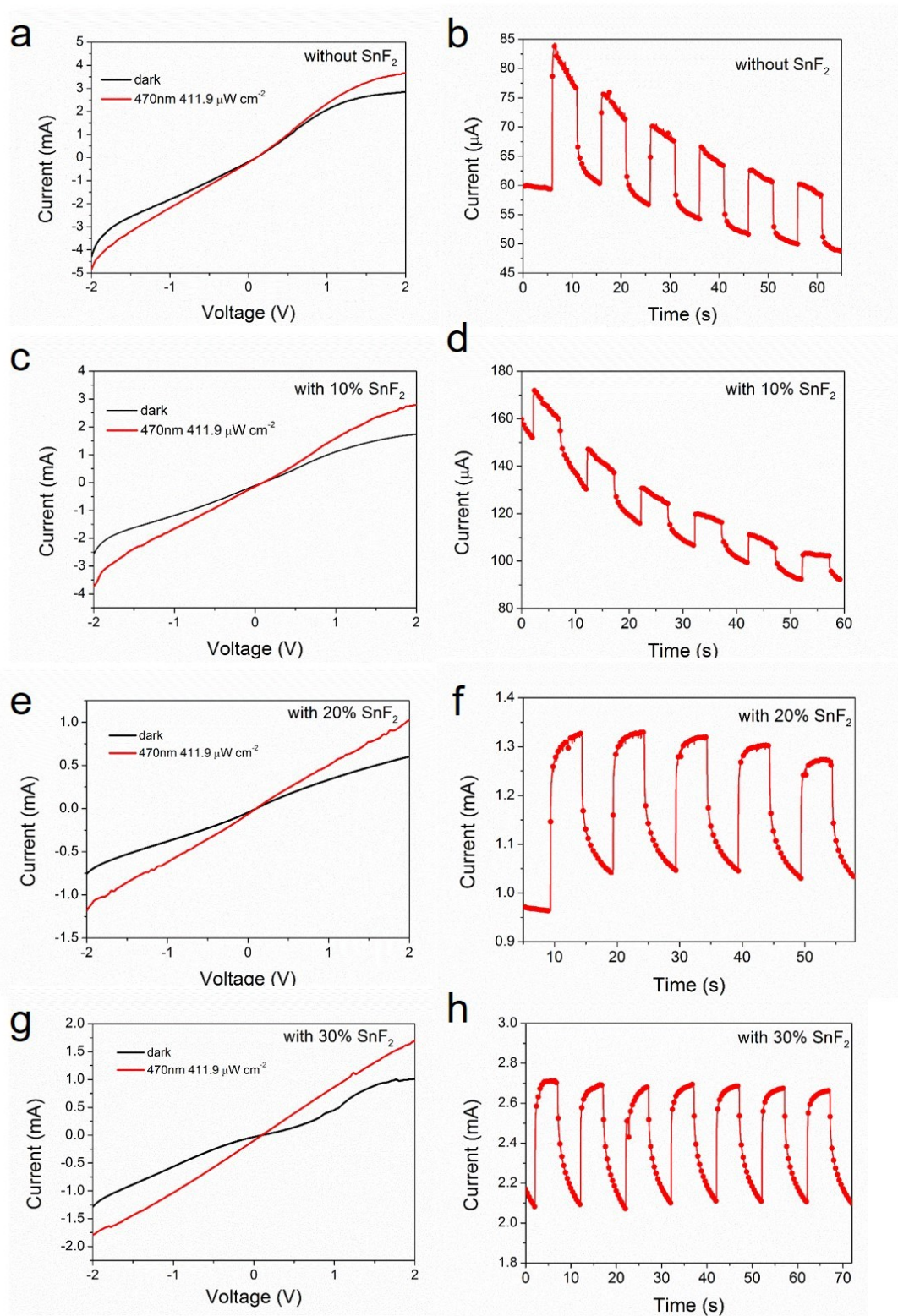


Fig. S10 I-V and I- T curves of the Au devices in dark or under 470nm illumination based on perovskite with different amount addition of SnF_2 .

Note: Without SnF_2 addition, the photocurrent decays with time under continuous 5 V bias voltage (Fig. S10b, d). The I-T curves in Fig. S10 was tested after many circles, so the current decayed to a low value in Fig. S10b, d. However, when adding 20~30 mol% SnF_2 , the current didn't decay with the time, so the value maintained on a high level (Fig. S10f, h). The reduced conductivity of $(\text{PEA})_2\text{SnI}_4$ film is shown in I-V curves (Fig. S10a, c, e, g) that the dark current under 5 V bias reduced from ~5 mA (Fig. S10a) to around 1 mA (Fig. S10e, g).

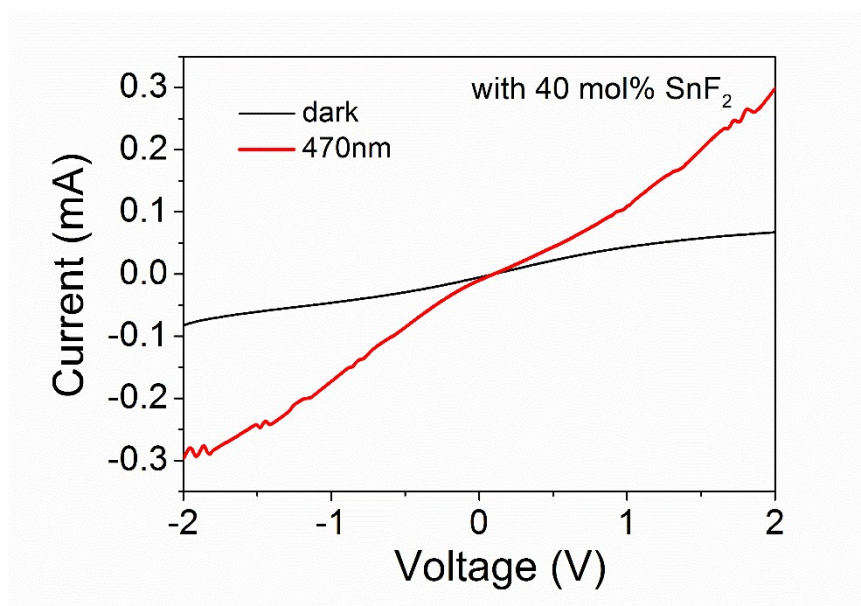


Fig. S11 *I-V* curves of the Au device in dark or under 470nm illumination based on perovskite with 40 mol% addition of SnF_2 .

Note: The photocurrent decreased significantly compared with devices with less SnF_2 (Fig. S10). Combined with film morphology of 40 mol% SnF_2 addition (Fig. S8d), the decreased current may be caused by bad film morphology.

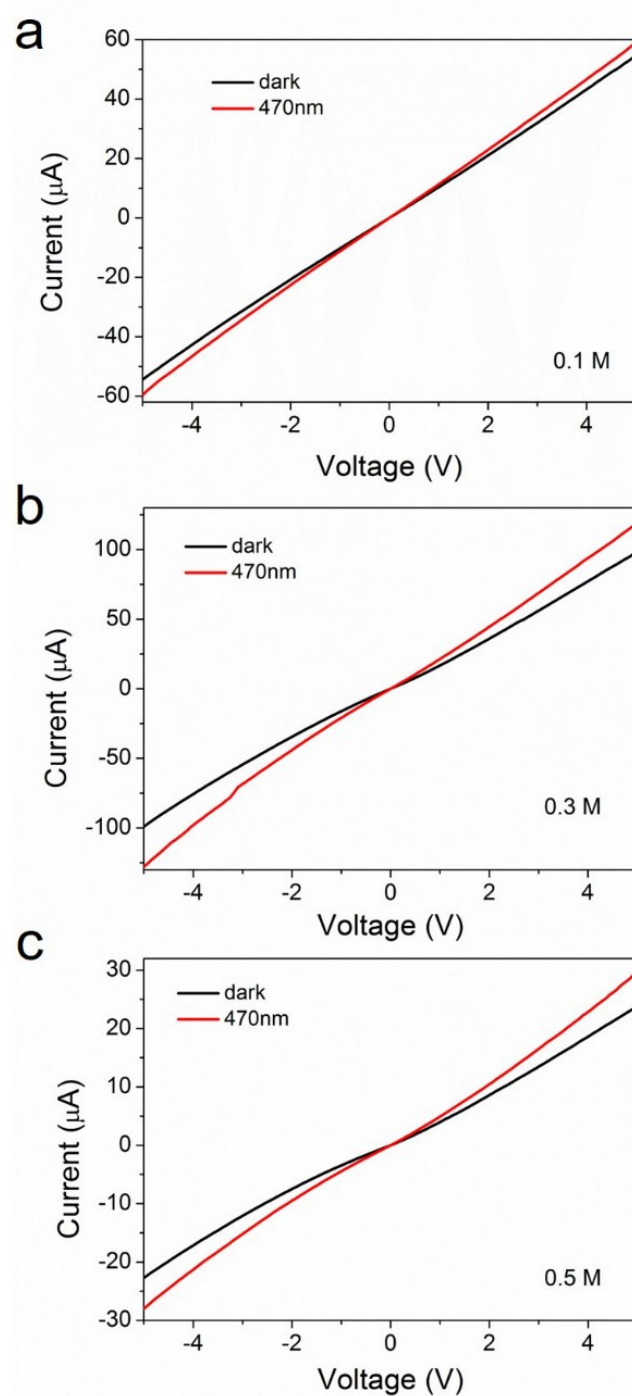


Fig. S12 I - V curves of rGO/(PEDOT:PSS) flexible devices in dark or under 470 nm illumination based on perovskite depositing from precursor solution with different concentration.

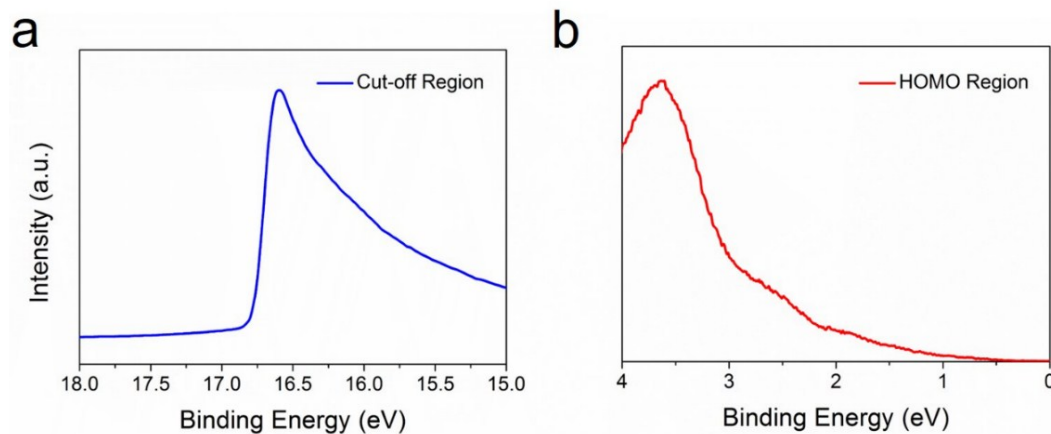


Fig. S13 UPS spectra of perovskite film with 30mol% SnF_2 . a) cut-off region, b) HOMO region.

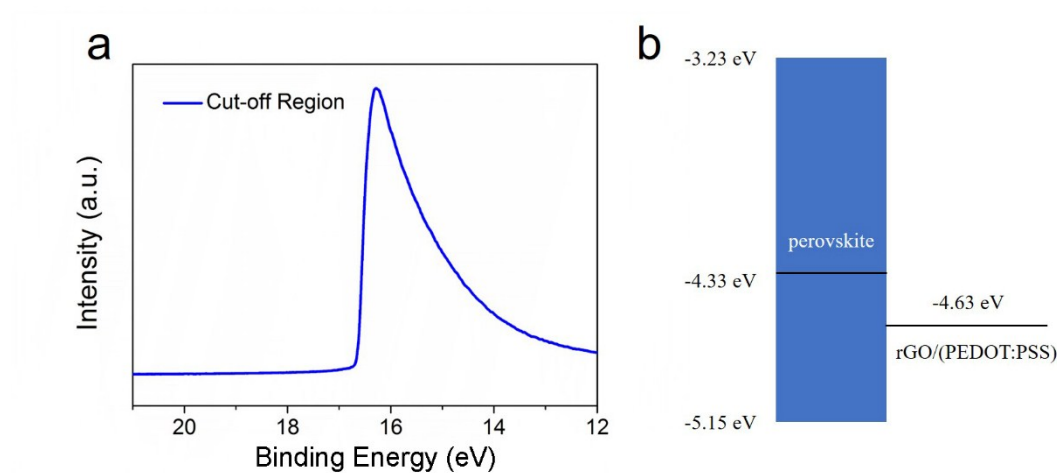


Fig. S14 a) UPS cut-off region spectrum of rGO/(PEDOT:PSS) film. b) Energy level diagram of $(\text{PEA})_2\text{SnI}_4$ perovskite, rGO/(PEDOT:PSS) and Au electrode.

Note: The work function of Au is 5.1 eV, which is closer to the HOMO level of $(\text{PEA})_2\text{SnI}_4$. Considering the hole dominated photocurrent in this device, using Au electrode can reduce the loss of holes. Besides, rGO/(PEDOT:PSS) electrode contained chemically reduced GO, which might cause more defects on the surface than vacuum deposited Au electrode. The recombination at perovskite/Au interface is less than that at perovskite/rGO-P60 interface.

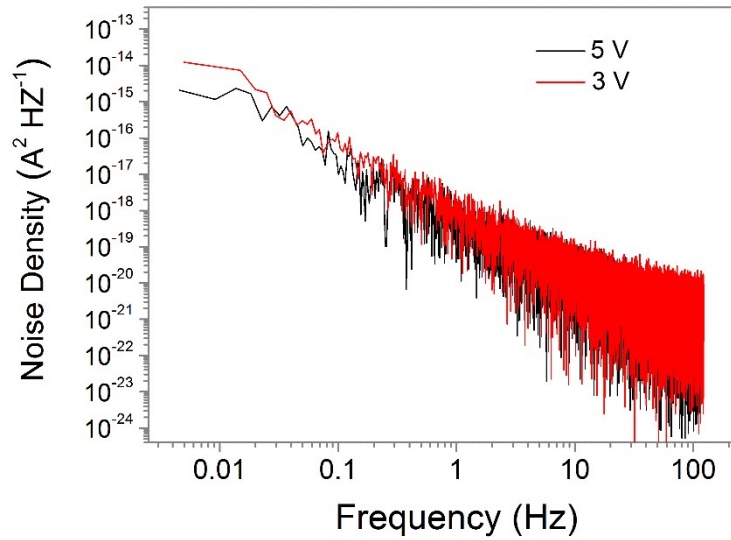


Fig. S15 Noise analysis of the flexible photoconductors measured under different bias voltage. The measured noise density was obtained from the Fast Fourier Transform of the dark current versus time.

Note: Figure S15 shows the measured noise density as a function of bias voltage obtained from the Fast Fourier Transform of the dark current versus time. The Sn perovskite device showed noise current (I_n) of $\sim 10 \text{ pA Hz}^{-1/2}$ at high frequencies.³ Specific detectivity (D^*) of the device was calculated by using the equation of $D^* = S^{1/2}/\text{NEP} = S^{1/2}/(I_n/R)$, where NEP is the noise equivalent power, I_n is the noise current in the unit of $\text{A Hz}^{-1/2}$. S is the effective area of the device, which is $0.18 \times 0.08 \text{ cm}^2$ here. R is the photoresponsivity of the device (16 A W^{-1}).

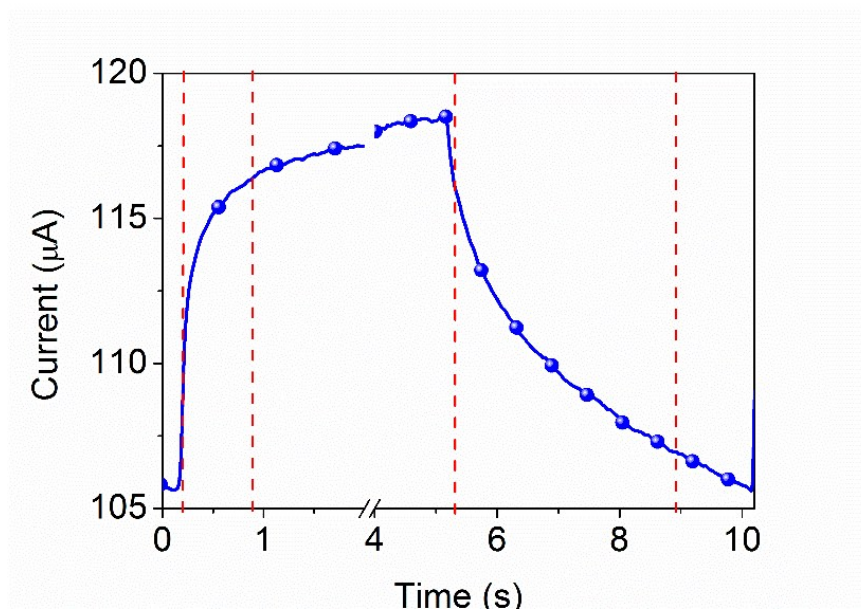


Fig. S16 An enlarged view of the temporal photocurrent response during on-off illumination switching with 5 s intervals

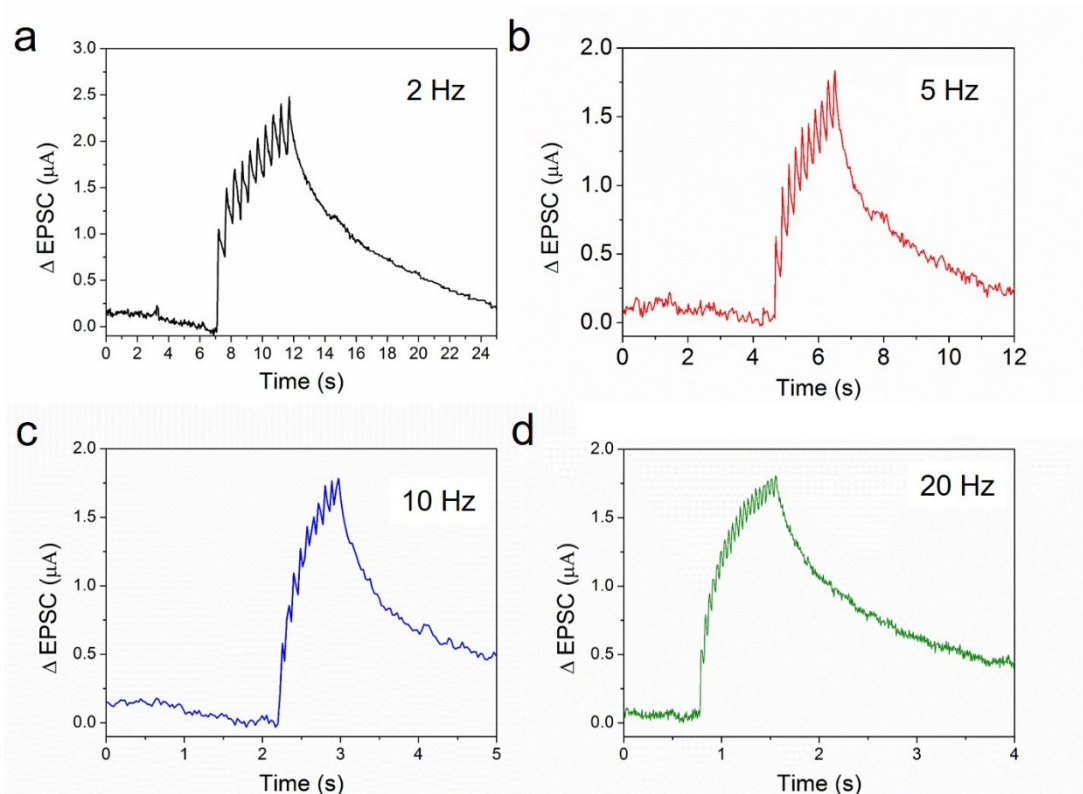


Fig. S17 EPSC changes triggered by using 10 light pulses with different frequency (20 pulses for 20 Hz).

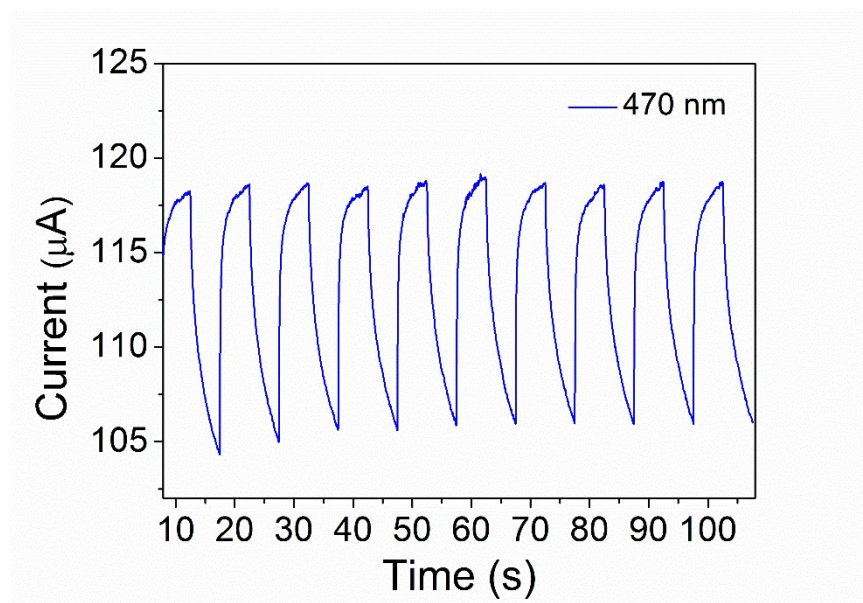


Fig. S18 I-T curve of the photoconductor under 470 nm illumination with on-off intervals of 5 s.

Note: The working stability of this synaptic device is essentially the stability of

photoresponse performance because the illumination of our LED is actually pulsed light with 50 Hz frequency. Fig. S18 is a long-time I-T curve of the photoconductor under 470 nm illumination with on-off intervals of 5 s. The photocurrent can maintain in the same value even after 10 cycles, which indicates good working stability of the device.

References

- [1] M. Wu, Y. Li, B. Yao, J. Chen, C. Li, G. Shi, *J. Mater. Chem. A*, 2016, **4**, 16213.
- [2] I. C. Smith, E. T. Hoke, D. Solis-Ibarra, M. D. McGehee and H. I. Karunadasa, *Angew. Chem*, 2014, **53**, 11232.
- [3] Q. Lin, A. Armin, P. L. Burn, P. Meredith, *Nat. Photon.*, 2015, **9**, 687.